Journal of Organometallic Chemistry 744 (2013) 35–40

Contents lists available at SciVerse ScienceDirect

Journal of Organometallic Chemistry

journal homepage: www.elsevier.com/locate/jorganchem

Reactivity of iridium(I) PNP amido complexes toward protonation and oxidation

Bjorn Askevold [b], Anja Friedrich [b], Magnus R. Buchner [b], Burhanshah Lewall [c], Alexander C. Filippou [c], Eberhardt Herdtweck [b], Sven Schneider [a,*]

[a] Institut für Anorganische Chemie, Georg-August-Universität Göttingen, Tammannstr. 4, 37077 Göttingen, Germany
[b] Department Chemie, Technische Universität München, Lichtenbergstr. 4, 85747 Garching, Germany
[c] Institut für Anorganische Chemie, Universität Bonn, Gerhard-Domagk Str. 1, 53121 Bonn, Germany

ARTICLE INFO

Article history:
Received 24 March 2013
Received in revised form
15 April 2013
Accepted 16 April 2013

Dedicated to Prof. Dr. Dr. h.c. mult. W. A. Herrmann on the occasion of his 65th birthday

Keywords:
Amido complex
Basicity
Oxidation

ABSTRACT

Iridium PNP amido complex [Ir(PMe$_3$){N(CH$_2$CH$_2$P^{i}Pr$_2$)$_2$}] (**3^{PMe3}**) was prepared in high yield starting from ethylene amine complex [Ir(C$_2$H$_4$){HN(CH$_2$CH$_2$P^{i}Pr$_2$)$_2$}]PF$_6$. The high nucleophilicity of the amido nitrogen atom is demonstrated by facile *N*-methylation with MeOTf. The *N*-basicity within the series [IrL{N(CH$_2$CH$_2$P^{i}Pr$_2$)$_2$}] (**3^{L}**; L = PMe$_3$, cyclooctene, CO) is quantified by determination of the corresponding amine complex pK_a values. Examination of chemical and electrochemical oxidation of **3^{L}** point toward decomposition of the primary oxidation product by ligand centered disproportionation. The strong dependence of the basicity and oxidation potentials on the nature of L is rationalized on the basis of 3c-4e N–M–L π-interactions.

1. Introduction

Covalently bound π-donor (e.g. amido) ligands are frequently used to stabilize complexes of early transition metals (TMs) in high oxidation states [1]. In contrast, low-valent, late TM amido complexes are much more rare [2]. Their distinct reactivity can be attributed to M–NR$_2$ bonding, particularly the lack of vacant metal *d*-orbitals with suitable symmetry, which prevents charge delocalization by N → M π-donation [3]. Hence, high *N*-centered basicity and nucleophilicity results, e.g. leading to the formation of bridging amido complexes. Coordinatively unsaturated alkylamides of these metals tend to decompose by β-H elimination [4]. The strong contribution of the energetically high-lying nitrogen lone pair to the HOMO also suggests amido ligand non-innocence upon oxidation as demonstrated by the characterization of a few molecular amides with predominant aminyl character [5,6]. These (electronic) structure/reactivity-relationships have been exploited in metal mediated or catalyzed processes, such as C–N cross coupling, bifunctional hydroelementation, or amine oxidation [7–9]. While the general reactivity trends are well understood, a lack of comprehensive studies, which allow for the estimation of secondary ligand effects, is apparent.

Anionic pincer ligands, such as the archetypal aryl PCP pincer {C$_6$H$_3$-2,6-(CH$_2$PR$_2$)$_2$}$^-$, have been popularized for catalysis owing to the high thermal stability and versatile structural control by steric adjustment of the substituents [10]. The variation of the central functional group, e.g. by introduction of a π-donor group as in disilylamido, diarylamido, or pyridine based PNP pincer ligands, allows for further control of the electronic structure [2b,11]. Our and other groups recently set out to explore the chemistry of complexes with highly π-basic alkyl- and vinylamido ligands derived from the chelating amine ligand HN(CH$_2$CH$_2$PR$_2$)$_2$ (*H*PNP^R; R = *i*-Pr, *t*-Bu) [12]. For example, we reported the synthesis of some square-planar d^8 amine complexes, [ML(*H*PNP^{iPr})]$^+$ (M = Ir, L = CO (**1^{CO}**), cyclooctene (**1^{COE}**), C$_2$H$_4$ (**1^{C2H4}**); M = Pd, L = Cl (**2^{Cl}**), Me (**2^{Me}**), Ph (**2^{Ph}**)), and the corresponding amido complexes [ML(PNP^{iPr})] (M = Ir, L = CO (**3^{CO}**), cyclooctene (**3^{COE}**), C$_2$H$_4$ (**3^{C2H4}**); M = Pd, L = Cl (**4^{Cl}**), Me (**4^{Me}**), Ph (**4^{Ph}**)) [13,14]. In the present paper, we present a study which is aimed at assessing the reactivity trends with

* Corresponding author. Fax: +49 551 3922582.
E-mail address: sven.schneider@chemie.uni-goettingen.de (S. Schneider).

0022-328X/$ – see front matter © 2013 Elsevier B.V. All rights reserved.
http://dx.doi.org/10.1016/j.jorganchem.2013.04.022

electrophiles and oxidizing agents as dependent on further secondary ligands.

2. Results and discussion

2.1. Syntheses and structural characterizations

[Ir(PMe$_3$)(*H*PNP^{iPr})]PF$_6$ (**1^{PMe3}**) was synthesized in high yield from ethylene complex **1^{C2H4}** and PMe$_3$ (Scheme 1). The corresponding dmso complex [Ir(OSMe$_2$)(*H*PNP^{iPr})]BPh$_4$ (**1^{dmso}**) was prepared directly from [IrCl(dmso)$_2$]$_2$, *H*PNP^{iPr}, and NaBPh$_4$. The NMR spectroscopic features of **1^{PMe3}** and **1^{dmso}** strongly resemble those of the related amine complexes **1^{CO}** and **1^{C2H4}**, indicating C_s symmetry on the NMR timescale as a result of the pyramidally coordinated nitrogen atom. The $^2J_{PP}$ coupling constant of **1^{PMe3}** (19 Hz) is in agreement with a mutual *cis* configuration of the PMe$_3$ ligand and the pincer ligand phosphine atoms, respectively. Reaction of **1^{PMe3}** with KO^{t}Bu gives the corresponding amido complex [Ir(PMe$_3$)(PNP^{iPr})] (**3^{PMe3}**) in high yield (Scheme 1). Deprotonation of the amine ligand effects C_{2v} symmetry on the NMR timescale, as expected for these square-planar amido complexes with three-coordinate nitrogen. All attempts to synthesize the corresponding amido complex from **1^{dmso}** were unsuccessful and resulted in complex mixtures of products, which were not further characterized.

The square-planar coordination geometry around the metal centers of **1^{PMe3}** and **3^{PMe3}** was also confirmed by single crystal X-ray diffraction (Fig. 1). Most structural parameters of **1^{PMe3}** and **3^{PMe3}** (Table 1) strongly resemble the respective ethylene and CO complexes [13a]. As for these previously reported examples, deprotonation of the nitrogen atom is accompanied by shortening of the Ir–N bond by more than 0.1 Å. The most apparent structural difference within the series of Ir^I amido complexes **3^L** (L = PMe$_3$, C$_2$H$_4$, CO) in comparison with Pd^{II} complexes **4^{Cl}**, **4^{Me}**, and [Pd(CN^{t}Bu){N(CH$_2$CH$_2$P^{i}Pr$_2$)$_2$}]PF$_6$ (**4^{CNtBu}**) is the more planar coordination around the amido nitrogen for Ir than for Pd, as expressed by the sum of bond angles around the nitrogen atoms (Ir: 355.7° (**3^{CO}**), 356.6° (**3^{C2H4}**), 353.0° (**3^{PMe3}**); Pd: 337.4° (**4^{Cl}**), 345.7° (**4^{Me}**), 343.2° (**4^{CNtBu}**)) [13a,14]. Planarization of the nitrogen atom coordination is a structural prerequisite for N–M π-bonding, indicating stronger π-interactions for **3^L** as compared with **4^R** in the solid state. However, conformational changes regarding pyramidalization around the nitrogen atom within this flexible ligand framework will exhibit a shallow potential energy surface.

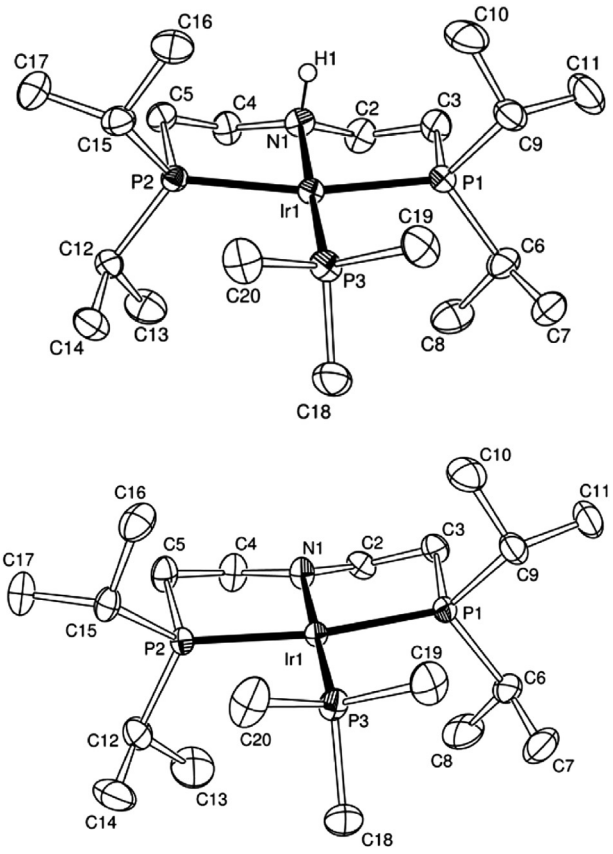

Fig. 1. Molecular structures of complexes **1^{PMe3}** (above, anion omitted) and **3^{PMe3}** (below) with thermal ellipsoids drawn at the 50% probability level (hydrogen atoms, except N–H) are omitted for clarity.

2.2. Reaction of 3^L with electrophiles

Complex **3^{PMe3}** reacts with MeOTf to give [Ir(PMe$_3$){MeN(CH$_2$CH$_2$P^{i}Pr$_2$)$_2$}]OTf (**5**), selectively (Scheme 1). Complex **5**

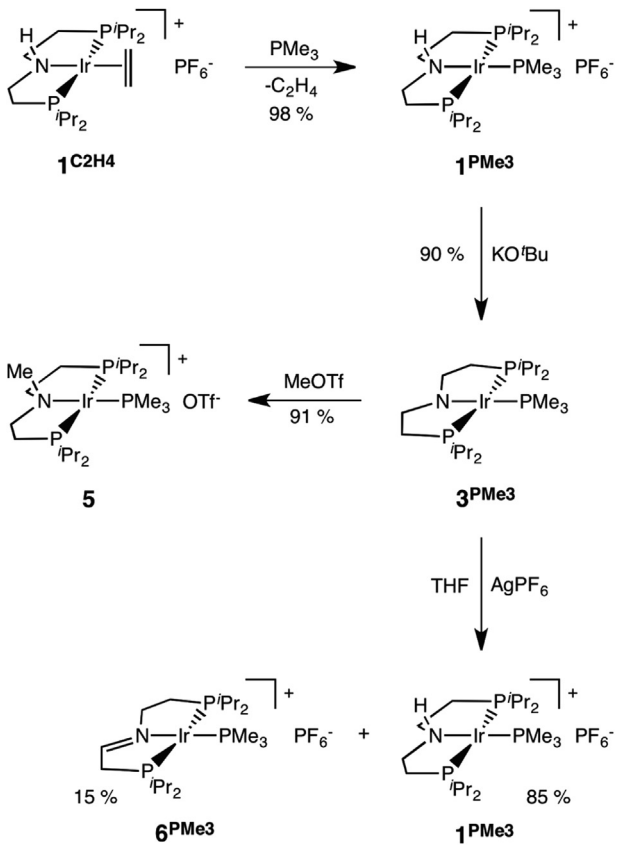

Scheme 1. Synthesis and reactivity of amido complex **3^{PMe3}**.

Table 1
Selected bond lengths and angles of **1^{PMe3}** and **3^{PMe3}** in the crystal.

	1^{PMe3}	**3^{PMe3}**
Bond lengths [Å]		
Ir1–N1	2.176(3)	2.069(2)
Ir1–P1	2.3079(9)	2.2892(7)
Ir1–P2	2.3033(9)	2.2764(7)
Ir1–P3	2.2309(9)	2.2225(7)
Bond angles [°]		
P1–Ir1–N1	82.04(8)	81.29(6)
P2–Ir1–N1	82.19(8)	81.67(6)
P3–Ir1–N1	178.07(8)	178.48(7)
P1–Ir1–P2	164.10(3)	162.89(3)

Table 2
pK_a values of $\mathbf{1}^{\mathbf{L}}$ in d^6-dmso and oxidation potentials of $\mathbf{3}^{\mathbf{L}}$ and of $\mathbf{1}^{\mathbf{PMe3}}$ (*vs.* $Fe(C_5Me_5)_2/Fe(C_5Me_5)_2^+$) at room temperature; ratio anodic/cathodic currents (I_p^a/I_p^c) in parantheses (electrolyte: THF, 0.1 M NBu_4PF_6; scan rate: 100 mV s^{-1}; $E_{1/2} = (E_a + E_c)/2$; n.m. = not measured).

L	pK_a[a]	$E^{I}_{1/2}$ [V][b]	$E^{II}_{1/2}$ [V][b]	$E^{III}_{1/2}$ [V][b]
PMe_3	22.0(1)	−0.66 (3.3)	−0.26 (1.0)	+0.53 (1.9)[c]
COE	16.0(4)	−0.06 (4.3)	+0.16 (1.0)	+0.80 (2.0)
CO	14.8(2)	+0.04 (3.1)	+0.40 (2.0)	+0.78 (2.0)

[a] Amine complexes $[IrL\{HN(CH_2CH_2P^iPr_2)_2\}]^+$ ($\mathbf{1}^{\mathbf{L}}$).
[b] Amido complexes $[IrL\{N(CH_2CH_2P^iPr_2)_2\}]$ ($\mathbf{3}^{\mathbf{L}}$).
[c] $E^{III}_{1/2}([IrL\{HN(CH_2CH_2P^iPr_2)_2\}]PF_6) = +0.52$ V (2.0).

was characterized by multinuclear NMR spectroscopy and elemental analysis. The singlet signals at 2.70 (^{1}H NMR) and 44.9 ppm (^{13}C NMR), respectively, can be assigned to the *N*-methyl group. The same reactivity was found for $\mathbf{4}^{\mathbf{Cl}}$ and other palladium(II) amido complexes [14,15]. In case of iridium(I), attack of *C*-electrophiles at the metal center instead of the amido nitrogen atom seems more likely as compared with Pd^{II}, considering the thermodynamic and kinetic accessibility of Ir(III) by oxidative addition to Ir^{I}. However, no indication for the formation of an iridium(III) methyl complex was found in the present case.

The *N*-centered Brønstedt basicity of $\mathbf{3}^{\mathbf{L}}$ (L = PMe_3, COE, CO) was quantified from equilibrium constants with suitable acids by NMR spectroscopy. As solvent, d_6-dmso was chosen to prevent contact ion formation and make use of the extensive reference pK_a data available for this solvent [16]. The corresponding amine ($\mathbf{1}^{\mathbf{L}}$) pK_a values derived in this way are provided in Table 2. Despite the relevance for catalysis, only few pK_a values of amine complexes in non-aqueous solvents were reported in the literature [17]. Within this series, the ligand in *trans*-position to the PNP nitrogen atom exhibits a strong influence on amine acidity, varying over a range of more than seven orders of magnitude. The data follows the expected trend: π-acceptor ligands like cyclooctene ($\mathbf{1}^{\mathbf{COE}}/\mathbf{3}^{\mathbf{COE}}$) and CO ($\mathbf{1}^{\mathbf{CO}}/\mathbf{3}^{\mathbf{CO}}$) stabilize the electron rich amido complexes resulting in considerably lower pK_a (see below). However, the large range of the pK_a values is remarkable in comparison with the ones derived for Pd complexes. There, both $\mathbf{2}^{\mathbf{Me}}$ (24.2(1)) and $\mathbf{2}^{\mathbf{Ph}}$ (23.2(1)) exhibit almost identical pK_a [14]. As indicated by the molecular structures (see above), more pronounced π-bonding for iridium(I) could be responsible.

The electronic structure of $\mathbf{3}^{\mathbf{CO}}$ was also examined by DFT computations (B3LYP/6-311 + G**) to evaluate the qualitative picture (Fig. 2). The π-interaction that mixes the nitrogen lone pair, the d_{xz} orbital, and the respective in-plane π*(CO)-orbital gives three molecular orbitals (HOMO-3, HOMO, and LUMO) that are occupied

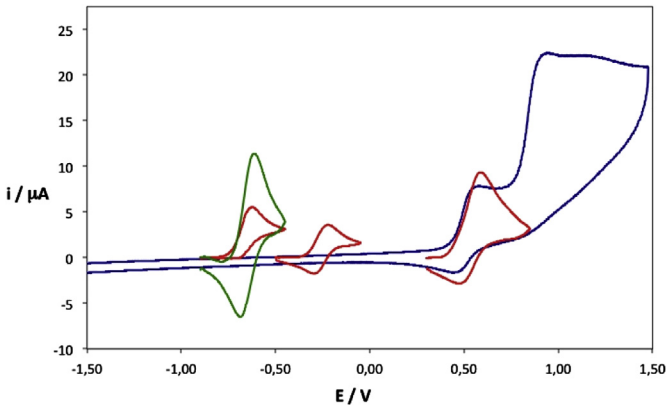

Fig. 3. Cyclic voltammograms (CVs) of complexes $\mathbf{3}^{\mathbf{PMe3}}$ and of $\mathbf{1}^{\mathbf{PMe3}}$ (*vs.* $Fe(C_5Me_5)_2/Fe(C_5Me_5)_2^+$) at room temperature (THF, 0.1 M NBu_4PF_6). Red: CVs of $\mathbf{3}^{\mathbf{PMe3}}$ at scan rate 100 mV s^{-1}. Green: CV of $\mathbf{3}^{\mathbf{PMe3}}$ at scan rate 800 mV s^{-1}. Blue: CV of $\mathbf{1}^{\mathbf{PMe3}}$ at scan rate 100 mV s^{-1}.

with four electrons. The HOMO exhibits strong N–Ir π-antibonding character, resulting in the absence of a net N–Ir π-bond. Importantly, $d_{xz} \rightarrow \pi^*(CO)$ backbonding stabilizes the HOMO in terms of a 3c-4e N–Ir-L *push–pull* π-interaction. Furthermore, the reactivity of $\mathbf{3}^{\mathbf{L}}$ as an *N*-nucleophile can be rationalized with the higher energy of this orbital, relative to the highest occupied, metal centered orbital (d_z2, HOMO-1).

2.3. Oxidation of $\mathbf{3}^{\mathbf{L}}$

We previously reported that chemical oxidation of palladium(II) amide $\mathbf{4}^{\mathbf{Ph}}$ with $AgPF_6$ in THF gives amine complex $\mathbf{2}^{\mathbf{Ph}}$ as major product and minor quantities of imine $[PdPh\{N(CHCH_2P^iPr_2)(CH_2CH_2P^iPr_2)\}]$ [14]. Deuterium labeling suggested the formation of transient radical cation $[PdPh(PNP^{iPr})]^+$ which decomposes by hydrogen atom transfer from the solvent and disproportionation of the chelate backbone to amine and imine complexes. Similarly, the reaction of iridium(I) amide $\mathbf{3}^{\mathbf{PMe3}}$ with $AgPF_6$, $[FeCp_2]PF_6$, or CPh_3PF_6, respectively, in THF (Scheme 1) results in the formation of $\mathbf{1}^{\mathbf{PMe3}}$ as major product (85% by ^{31}P NMR). As in case of Pd, the minor product (15%) is assigned to imine complex $[Ir(PMe_3)\{N(CHCH_2P^iPr_2)(CH_2CH_2P^iPr_2)\}][PF_6]$ ($\mathbf{6}^{\mathbf{PMe3}}$) on the basis of ^{31}P and ^{1}H NMR spectroscopy. Unfortunately, $\mathbf{6}^{\mathbf{PMe3}}$ could not be isolated in pure form, to date.

The oxidation of the iridium(I) PNP amides $\mathbf{3}^{\mathbf{L}}$ (L = PMe_3, COE, CO) was further examined by cyclic voltammetry (CV) in a THF/

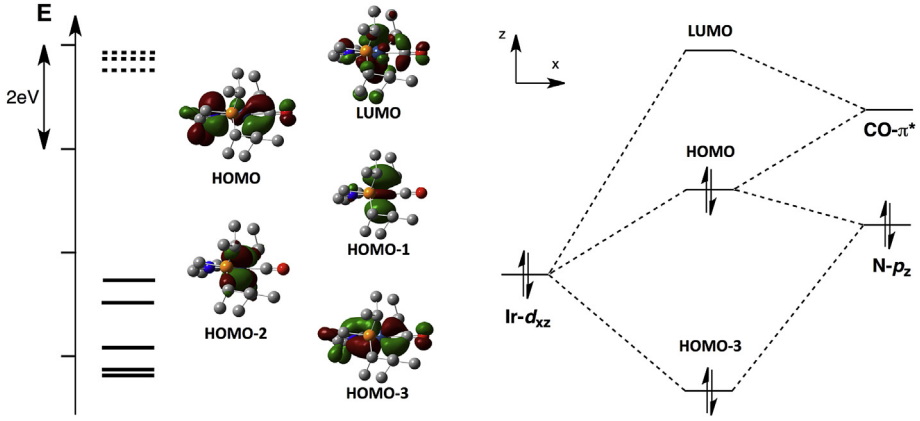

Fig. 2. Frontier Kohn–Sham orbital scheme (left), graphical orbital representations (center) and three center π-interaction (right) for $\mathbf{3}^{\mathbf{CO}}$.

$N(^nBu)_4PF_6$ electrolyte. The first oxidation ($1e^-$) is characterized by an anodic wave at $E^I_{1/2}$ (Table 1 and Fig. 3), which is strongly dependent on the ligand L. As expected, $\mathbf{3^{PMe3}}$ is oxidized at considerably more negative potential compared with $\mathbf{3^{COE}}$ and $\mathbf{3^{CO}}$, which carry strong π-acceptor ligands instead of PMe_3. Irreversibility of this oxidation process at scan rates of 100 mV s^{-1} is indicated by the ratios of the anodic and cathodic currents, yet becoming increasingly quasireversible at higher scan rates. A second oxidation at higher potential ($E^{II}_{1/2}$) was found to be quasi-reversible at scan rates of 100 mV s^{-1} for $\mathbf{3^{PMe3}}$ and $\mathbf{3^{COE}}$ but irreversible for $\mathbf{3^{CO}}$ at all experimental conditions (100–600 mV s^{-1}). Finally, all three compounds exhibit an irreversible anodic wave at higher potentials ($E_{1/2}{}^{III}$). For $\mathbf{3^{PMe3}}$, this last redox process was assigned to the oxidation of the corresponding amine complex $\mathbf{1^{PMe3}}$ by comparison with the CV of an original sample. The results from electrochemical and chemical oxidation are rationalized with an ECEE mechanism on the electrochemical timescale [18]. The initial radical from one-electron oxidation of $\mathbf{3^L}$ disproportionates by ligand backbone hydrogen transfer. For $\mathbf{3^{PMe3}}$, the resulting amine ($\mathbf{1^{PMe3}}$) and imine ($\mathbf{6^{PMe3}}$) complexes were detected by NMR spectroscopy after chemical oxidation and $\mathbf{1^{PMe3}}$ was unambiguously detected as product from electrochemical oxidation ($E^{III}_{1/2}$), as well. Hence, the redox process at potential $E^{II}_{1/2}$ is tentatively assigned to the imine complexes $\mathbf{6^L}$.

3. Conclusions

Electron rich metal amido complexes are particularly interesting compounds owing to their distinct ligand centered basicity and redox chemistry. In this context, a series of square planar iridium(I) dialkylamido complexes $\mathbf{3^L}$ (L = PMe_3, COE, CO) was probed with respect to the reactivity toward electrophiles and oxidation. $\mathbf{3^L}$ readily reacts with *C*-electrophiles or Brønstedt acids upon *N*-alkylation and −protonation, respectively. In contrast to analogous palladium complexes, the amine pK_a values are strongly dependent on the *N*-trans ligand allowing for facile tuning of this property. Similarly, the oxidation of $\mathbf{3^L}$ exhibits a strong dependence on the π-acceptor ability of L. Chemical and electrochemical oxidation studies indicate decomposition of the transient amido radical by ligand-centered disproportionation. However, while ligand-centered redox processes are prevalent, the electrochemical potentials can be effectively tuned by choice of the appropriate Ir/auxiliary ligand platform. This strong influence of the ligand in *trans*-position is attributed to an N–M–L 3*c*-4*e* push–pull interaction, providing guidelines for the design of cooperative or redox-catalysts.

4. Experimental section

4.1. Materials and methods

All experiments were carried out under an atmosphere of argon using Schlenk and glove-box techniques. The solvents were dried over Na/benzophenone (THF) and distilled under argon or dried and deoxygenated by passing through columns packed with activated alumina and Q5, respectively. C_6D_6 and d_8-THF were dried by distillation from Na/K alloy. d_6-acetone and dmso were stirred over 4 Å molecular sieve and distilled from B_2O_3 (d_6-acetone) or CaH_2 (dmso), respectively. All deuterated solvents were deoxygenated by three *freeze–pump–thaw* cycles. KO^{t}Bu was purchased from VWR and sublimed prior to use. $AgPF_6$ (ABCR), $[FeCp_2]PF_6$ (Aldrich), CPh_3PF_6 (VWR) and MeOTf (Aldrich) were used as purchased. $[IrCl(dmso)_2]_2$ and $\mathbf{1^{C2H4}}$ were prepared according to published procedures [13a,19].

4.2. Analytical methods

Elemental analyses were obtained from the Microanalytical Laboratory of Technische Universität München. The IR spectra were recorded on a Jasco FT/IR-460 PLUS spectrometer as nujol mulls between KBr plates. NMR spectra were recorded on Jeol Lambda 400 spectrometers at room temperature and calibrated to the residual proton resonance and the natural abundance ^{13}C resonance of the solvent (C_6D_6, δ_H = 7.16 ppm, δ_C = 128.1 ppm; d_6-dmso, δ_H = 2.50 ppm, δ_C = 39.5 ppm, d_8-THF, δ_H = 1.73 and 3.58 ppm, δ_C = 25.3 and 67.2 ppm, d_6-acetone δ_H = 2.05 ppm, δ_C = 29.8 ppm and 206.3). ^{31}P NMR chemical shifts are reported relative to external phosphoric acid (δ = 0.0 ppm). IR peak intensities are abbreviated as: m (medium), s (strong). NMR Signal multiplicities are abbreviated as: s (singlet), d (doublet), t (triplet), vt (virtual triplet), sp (septet), m (multiplet), br (broad). Cyclic voltammograms were recorded with a glassy carbon working electrode, a platinum wire counter electrode, and a $Fe(C_5Me_5)_2/Fe(C_5Me_5)_2^+$ reference electrode. The potential of the reference electrode *vs.* $Fe(C_5H_5)_2/Fe(C_5H_5)_2^+$ (ΔE = +466 mV) was derived by external standard measurements.

4.2.1. pK_a determinations

The amido complexes $\mathbf{3^L}$ and an equimolar amount of a corresponding acid with suitable pK_a ($\mathbf{3^{CO}}$ and $\mathbf{3^{COE}}$: benzimidazole; $\mathbf{3^{PMe3}}$: 2-pyrrolidinone) were dissolved in 0.6 mL of d_6-dmso. Due to fast proton exchange on the NMR time scale one peak resulted in the ^{31}P NMR with a chemical shift δ_{meas} that was located between those of pure $\mathbf{1^L}$ (δ_{1L}) and $\mathbf{3^L}$ (δ_{3L}) in d_6-dmso. The equilibrium molar fractions of $\mathbf{3^L}$ (x_{3L}) and the corresponding $\mathbf{1^L}$ (x_{1L}) conjugate acid cation were derived using:

$$\delta_{meas} = X_{1L}\delta_{1L} + X_{3L}\delta_{3L} \quad (1)$$

$$X_{1L} + X_{3L} = 1 \quad (2)$$

pK_a values were calculated from the equilibrium constant (K_{eq}) using the following equations (pK_a(2-pyrrolidinone) = 24.2; pK_a(benzimidazole) = 16.4) [20]:

$$K_{eq} = X^2_{3L}/X^2_{1L} \quad (3)$$

$$pK_a(1^L) = pK_a(ref) - \log(K_{eq}) \quad (4)$$

4.3. Syntheses

4.3.1. [Ir(PMe$_3$)(HPNP^{iPr})]PF$_6$ ($\mathbf{1^{PMe3}}$)

$[Ir(C_2H_4)(PNP)^H][PF_6]$ ($\mathbf{1^{C2H4}}$) (0.029 g; 0.043 mmol) is dissolved in THF (5 mL) and PMe_3 (1.0 M in THF; 0.060 mL; 1.4 eq) added via syringe. The yellow solution is stirred for 10 min, filtered, and pentanes (20 mL) added to give a yellow precipitate. The product is filtered off, washed with 10 mL pentanes and dried *i. vac.* Yield: 0.030 g (0.042 mmol, 98%). Anal. Calcd. for $C_{19}H_{46}F_6IrNP_4$ (718.68): C, 31.75; H, 6.45; N, 1.95. Found: C, 31.65; H, 6.06; N, 1.88. IR (Nujol, cm^{-1}) ν = 3240 (m, N–H). NMR (C_6D_6/d_8-THF, r.t., [ppm]) ^1H NMR (399.8 MHz): δ = 0.93 (m, 18H, CH_3), 1.09 ($A_3MXX'M'A_3$, N = $|^3J_{HP} + {}^5J_{HP}|$ = 16.4 Hz, $^3J_{HH}$ = 7.2 Hz, 6H, CH_3), 1.24 (d, 9H, $^2J_{HP}$ = 8.0 Hz, P(CH_3)$_3$), 1.63 (m, 2H, PCH_2), 1.72–1.98 (m, 8H, PCH_2, $CH(CH_3)_2$, NCH_2), 3.21 (m, 2H, NCH_2), 4.50 (br, 1H, N*H*). ^{13}C {^1H} NMR (100.6 MHz): δ = 17.6 (s, CH_3), 18.4 (s, CH_3), 20.1 (s, CH_3), 20.4 (s, CH_3), 23.2 (d, J_{CP} =36.0 Hz, P(CH_3)$_3$), 25.1 (AMXM′A′, N = $|^1J_{CP} + {}^3J_{CP}|$ = 12.2 Hz,

$^3J_{CP}$ = 3.1 Hz, PCH$_2$), 26.1 (AXX′A′, N = |$^1J_{CP}$ + $^3J_{CP}$| = 14.5 Hz, CH(CH$_3$)$_2$), 27.7 (AXX′A′, N = |$^1J_{CP}$ + $^3J_{CP}$| = 13.8 Hz, CH(CH$_3$)$_2$), 55.4 (s, NCH$_2$). ^{31}P {^{1}H} NMR (161.8 MHz): δ = 56.5 (d, $^2J_{PP}$ = 18.8 Hz, P^{i}Pr$_2$), −45.5 (d, $^2J_{PP}$ = 18.8 Hz, P(CH$_3$)$_3$), −143.0 (sp, $^1J_{PF}$ = 712.0 Hz, PF$_6$).

4.3.2. [Ir(SOMe$_2$)(HPNP^{iPr})]BPh$_4$ (**1^{dmso}**)

HN(CH$_2$CH$_2$P^{i}Pr$_2$)$_2$ (0.135 g; 0.443 mmol) in THF (5 mL) is added to a mixture of [IrCl(dmso)$_2$]$_2$ (0.170 g; 0.221 mmol) and NaBPh$_4$ (0.152 g; 0.443 mmol) in THF (5 mL). The solution is stirred for 1 h at room temperature and filtered. The yellow, microcrystalline product is precipitated by addition of diethylether (10 mL) and pentanes (5 mL), filtered off, and dried *i. vac.* Yield: 0.318 g (0.355 mmol, 80%). Anal. Calcd. for C$_{42}$H$_{63}$BIrNOP$_2$S (895.00): C, 56.36; H, 7.10; N, 1.57. Found: C, 56.86; H, 6.99; N, 1.30. IR (Nujol, cm^{-1}) ν = 3181 (s, N–H). NMR (d_8-THF, r.t., [ppm]) ^{1}H NMR (399.8 MHz): δ = 1.16 (A$_3$MXX′M′A$_3$′, N = |$^3J_{HP}$ + $^5J_{HP}$| = 14.0 Hz, $^3J_{HH}$ = 7.2 Hz, 6H, CH$_3$), 1.24 (A$_3$MXX′M′A$_3$′, N = |$^3J_{HP}$ + $^5J_{HP}$| = 14.0 Hz, $^3J_{HH}$ = 7.2 Hz, 6H, CH$_3$), 1.31 (m, 12H, CH$_3$), 1.46 (m, 2H, PCH$_2$), 1.96 (m, 2H, PCH$_2$), 2.15 (m, 2H, NCH$_2$), 2.35 (m, 2H, CH(CH$_3$)$_2$), 2.45 (m, 2H, CH(CH$_3$)$_2$), 2.78 (m, 2H, NCH$_2$), 3.36 (s, 6H, OS(CH$_3$)$_2$), 4.47 (br, 1H, NH), 6.72 (t, $^3J_{HH}$ = 7.2 Hz, 4H, B(C$_6$H$_5$)$_4$), 6.86 (t, $^3J_{HH}$ = 7.2 Hz, 8H, B(C$_6$H$_5$)$_4$), 7.28 (br, 8H, B(C$_6$H$_5$)$_4$). ^{13}C {^{1}H} NMR (100.6 MHz): δ = 17.1 (s, CH$_3$), 17.9 (s, CH$_3$), 19.3 (s, CH$_3$), 19.6 (s, CH$_3$), 23.6 (AXX′A′, N = |$^1J_{CP}$ + $^3J_{CP}$| = 13.0 Hz, PCH$_2$), 24.4 (m, CH(CH$_3$)$_2$), 26.7 (AXX′A′, N = |$^1J_{CP}$ + $^3J_{CP}$| = 14.5 Hz, CH(CH$_3$)$_2$), 53.3 (s, OS(CH$_3$)$_2$), 55.7 (br, NCH$_2$), 120.99 (s, B(C$_6$H$_5$)$_4$), 124.8 (s, B(C$_6$H$_5$)$_4$), 136.3 (s, B(C$_6$H$_5$)$_4$), 164.3 (q, $^1J_{CB}$ = 48.9 Hz, B(C$_6$H$_5$)$_4$). ^{31}P {^{1}H} NMR (161.8 MHz): δ = 58.13 (s, P^{i}Pr$_2$). ^{11}B {^{1}H} NMR (128.3 MHz): δ = −7.54 (s, B(C$_6$H$_5$)$_4$).

4.3.3. [Ir(PMe$_3$)(PNP^{iPr})] (**3^{PMe3}**)

1^{PMe3} (0.200 g; 0.224 mmol) and KO^{t}Bu (0.025 g; 0.223 mmol) were dissolved in THF (10 mL) and stirred for 10 min at room temperature. The solvent is evaporated and the residue is extracted with pentanes. After filtration, crystallization at −20 °C gives **3^{PMe3}** as orange crystals, which are filtered off and dried *i. vac*. Yield: 0.115 g (0.201 mmol, 90%). Anal. Calcd. for C$_{19}$H$_{45}$IrNP$_3$ (572.71): C, 39.85; H, 7.92; N, 2.45. Found: C, 40.00; H, 8.46; N, 2.49. NMR (C$_6$D$_6$, r.t., [ppm]) ^{1}H NMR (399.8 MHz): δ = 1.11 (A$_6$M$_2$XX′M$_2$′A$_6$′, N = |$^3J_{HP}$ + $^5J_{HP}$| = 12.8 Hz, $^3J_{HH}$ = 6.8 Hz, 12H, CH(CH$_3$)$_2$), 1.20 (A$_6$M$_2$XX′M$_2$′A$_6$′, N = |$^3J_{HP}$ + $^5J_{HP}$| = 15.2 Hz, $^3J_{HH}$ = 7.6 Hz, 12H, CH(CH$_3$)$_2$), 1.54 (d, $^2J_{HP}$ = 6.8 Hz, 9H, P(CH$_3$)$_3$), 1.85 (m, 4H, PCH$_2$), 1.96 (m, 4H, CH(CH$_3$)$_2$), 3.43 (m, 4H, NCH$_2$). ^{13}C {^{1}H} NMR (100.6 MHz): δ = 18.1 (s, CH$_3$), 20.3 (s, CH$_3$), 25.9 (d, $^1J_{CP}$ = 29.2 Hz, P(CH$_3$)$_3$), 26.6 (A$_2$XX′A′$_2$, N = |$^1J_{HP}$ + $^3J_{HP}$| = 13.1 Hz, CH(CH$_3$)$_2$), 28.6 (A$_2$MXM′A′$_2$, N = |$^1J_{HP}$ + $^3J_{HP}$| = 12.3 Hz, $^3J_{CP}$ = 5.3 Hz PCH$_2$), 62.6 (s (br), NCH$_2$). ^{31}P {^{1}H} NMR (161.8 MHz): δ = 68.1 (d, $^2J_{PP}$ = 18.3 Hz, P^{i}Pr$_2$), −55.2 (t, $^2J_{PP}$ = 18.3 Hz, P(CH$_3$)$_3$).

4.3.4. [Ir(PMe$_3$)(MePNP^{iPr})]OTf (**5**)

MeOTf (4.7 mg, 3.2 μL, 28 μmol) is added to a solution of [Ir(PMe$_3$)(PNP^{iPr})] (**3^{PMe3}**) (15.3 mg, 28 μmol) in toluene (2 mL) and stirred for 30 min until a yellow solid is formed. After removing of all volatiles, the product is washed twice with diethylether and dried *i. vac.* to give microcrystalline, yellow **5**. Yield 19 mg (0.026 mmol; 91%). Anal. Calcd. for C$_{21}$H$_{48}$F$_3$IrNO$_3$P$_3$S (736.81): C, 34.23; H, 6.57; N, 1.90; S, 4.35. Found: C, 33.79; H, 6.20; N, 1.91; S, 4.32. NMR (d_6-acetone, r.t., [ppm]) ^{1}H NMR (399.8 MHz): δ = 1.24–1.43 (m, 24 H, CH$_3$), 1.71 (d, $^2J_{PH}$ = 8.8 Hz, 9H, P(CH$_3$)$_3$), 2.25–2.31 (m, 4H, PCH$_2$), 2.25–2.31 (m, 4H, PCH$_2$), 2.34–2.41 (m, 2H, CH(CH$_3$)$_2$), 2.46–2.54 (m, 2H, CH(CH$_3$)$_2$), 2.70 (s, 3H, NCH$_3$), 2.81–2.91 (m, 2H, NCH$_2$), 2.99–3.11 (m, 2H, NCH$_2$). ^{13}C {^{1}H} NMR (100.6 MHz): δ = 16.7 (s, CH$_3$), 18.8 (s, CH$_3$), 20.0 (s, CH$_3$), 20.8 (m, PCH$_2$), 22.6 (d, PCH$_3$, $^1J_{CP}$ = 37.6 Hz), 23.1 (m, CH(CH$_3$)$_2$), 25.1 (m, CH(CH$_3$)$_2$), 44.9 (s, NCH$_3$), 64.4 (s, NCH$_2$). ^{31}P {^{1}H} NMR (161.8 MHz): δ = −47.6 (t, $^2J_{PP}$ = 18.8 Hz, P(CH$_3$)), 53.8 (d, $^2J_{PP}$ = 18.8 Hz, P^{i}Pr$_2$), ^{19}F NMR (376.2 MHz): δ = −78.7 (s, SO$_3$CF$_3$).

4.3.5. Chemical oxidation of **3^{PMe3}** in THF

3^{PMe3} (5 mg, 8.7 μmol) is dissolved in THF (0.5 mL) in a J-Young NMR tube and AgPF$_6$ (2.2 mg, 8.7 μmol) is added at room temperature. Immediately, the orange solution turns dark red and a black precipitate forms (Ag). The starting material is quantitatively converted to a mixture of **1^{PMe3}** (85%) and another compound (15%) that was assigned to [Ir(PMe$_3$)(N(CHCH$_2$P^{i}Pr$_2$)(CH$_2$CH$_2$P^{i}Pr$_2$))] (**7^{PMe3}**), based on NMR data: (d_8-THF, r.t., [ppm]) ^{1}H NMR (399.8 MHz): δ = 3.77 (m, 2H, NCHCH$_2$), 8.71 (d, $^3J_{HH}$ = 24.1 Hz, 1H, NCHCH$_2$). ^{31}P{^{1}H} NMR (161.8 MHz): δ = −43.9 (t, $^2J_{PP}$ = 19.8 Hz, P(CH$_3$)), 59.0 (dd, $^2J_{PP}$ = 19.8 Hz, $^2J_{PP}$ = 288.3 Hz, P^{i}Pr$_2$), 62.4 (dd, $^2J_{PP}$ = 18.8 Hz, $^2J_{PP}$ = 295.2 Hz, P^{i}Pr$_2$).

Upon using [FeCp$_2$]PF$_6$ (2.9 mg, 8.7 μmol) or CPh$_3$PF$_6$ (3.4 mg, 8.7 μmol) as oxidants the same observations are made.

4.4. Computational methods

DFT calculations on complex **3^{CO}** were performed with GAUSSIAN03 RevC.02 using the B3LYP functional [21,22]. Geometry optimizations were run without symmetry or internal coordinate constraints using the Stuttgart-RSC-ECP and corresponding valence basis set for iridium and all-electron split valence triple-ζ basis set 6-311 + G** for all other elements [23,24]. The optimized structure is in good agreement with the experimental molecular structure from X-ray diffraction and was verified as being a true minimum on the potential surface by the absence of negative eigenvalues in the vibrational frequency analysis. Orbitals were visualized with GaussView via cube files generated from formatted checkpoint files [25].

4.5. Single crystal X-ray structure determinations

Compound **1^{PMe3}**: Crystal data: formula: C$_{19}$H$_{46}$F$_6$IrNP$_4$; M_r = 718.67; crystal color and shape: orange fragment, crystal dimensions: 0.46 × 0.51 × 0.51 mm; crystal system: monoclinic; space group: *C*2/*c* (no. 15); *a* = 14.7502(6), *b* = 14.1777(4), *c* = 27.5450(11) Å, β = 99.002(3)°; *V* = 5689.4(4) Å^3; *Z* = 8; μ(Mo$_{K\alpha}$) = 4.966 mm^{-1}; ρ_{calcd} = 1.678 g cm^{-3}; θ-range = 4.00–26.80°; data collected: 38361; independent data [I_o>2σ(I_o)/all data/R_{int}]: 5102/5995/0.056; data/restraints/parameter: 5995/0/295; *R*1 [I_o>2σ(I_o)/all data]: 0.0259/0.0329; *wR*2 [I_o>2σ(I_o)/all data]: 0.0619/0.0638; GOF = 1.035; $\Delta\rho_{max/min}$: 2.21/−1.18 eÅ^{-3}. Compound **3^{PMe3}**: Crystal data: formula: C$_{19}$H$_{45}$IrNP$_3$; M_r = 572.69; crystal color and shape: orange fragment, crystal dimensions: 0.30 × 0.46 × 0.61 mm; crystal system: monoclinic; space group: *P*2$_1$/*c* (no. 14); *a* = 10.1460(4), *b* = 14.3405(5), *c* = 16.9529(8) Å, β = 97.606(4)°; *V* = 2444.92(17) Å^3; *Z* = 4; μ(Mo$_{K\alpha}$) = 5.660 mm^{-1}; ρ_{calcd} = 1.556 g cm^{-3}; θ-range = 4.05–26.81°; data collected: 35823; independent data [I_o>2σ(I_o)/all data/R_{int}]: 5049/5169/0.058; data/restraints/parameter: 5169/0/229; *R*1 [I_o>2σ(I_o)/all data]: 0.0207/0.0217; *wR*2 [I_o>2σ(I_o)/all data]: 0.0454/0.0458; GOF = 1.272; $\Delta\rho_{max/min}$: 0.87/−0.74 eÅ^{-3}.

Acknowledgments

The authors thank the Deutsche Forschungsgemeinschaft (Emmy-Noether Programm SCHN950/2-1) and the IDK NanoCat for funding.

Appendix A. Supplementary material

CCDC 929265 and 929266 contain the supplementary crystallographic data for this paper. This data can be obtained free of

charge from The Cambridge Crystallographic Data Centre via www.ccdc.cam.ac.uk/data_request/cif.

Appendix B. Supplementary data

Supplementary data related to this article can be found at http://dx.doi.org/10.1016/j.jorganchem.2013.04.022.

References

[1] (a) R. Kempe, Angew. Chem. 112 (2000) 478;
(b) M. Lappert, P. Power, A. Protchenko, A. Seeber, Metal Amide Chemistry, Wiley, Chichester, 2009.
[2] (a) H.E. Brzynda, W. Tam, Chem. Rev. 88 (1988) 1163;
(b) M.D. Fryzuk, C.D. Montgomery, Coord. Chem. Rev. 95 (1989) 1;
(c) M.D. Roundhill, Chem. Rev. 92 (1992) 1;
(d) R.G. Bergman, Polyhedron 14 (1995) 3227.(e) J.R. Fulton, A.W. Holland, D.J. Fox, R.G. Bergman, Acc. Chem. Res. 35 (2002) 44;
(f) T.B. Gunnoe, Eur. J. Inorg. Chem. (2007) 1185.
[3] (a) K.G. Caulton, New J. Chem. 18 (1994) 25;
(b) P.L. Holland, R.A. Andersen, R.G. Bergman, Comments Inorg. Chem. 21 (1999) 115.
[4] (a) S.E. Diamond, F. Mares, J. Organomet. Chem. 142 (1977) C55;
(b) J.F. Hartwig, J. Am. Chem. Soc. 118 (1996) 7010.(c) J.F. Hartwig, S. Richards, D. Baranano, F. Paul, J. Am. Chem. Soc. 118 (1996) 3626;
(d) S. Wagaw, R.A. Rennels, S.L. Buchwald, J. Am. Chem. Soc. 119 (1997) 8451.
[5] (a) F.N. Penkert, T. Weyhermüller, E. Bill, P. Hildebrandt, S. Lecomte, K. Wieghardt, J. Am. Chem. Soc. 122 (2000) 9663;
(b) T. Büttner, J. Geier, G. Frison, J. Harmer, C. Calle, A. Schweiger, H. Schönberg, H. Grützmacher, Science 307 (2005) 235;
(c) D. Adhikari, S. Mossin, F. Basuli, J.C. Huffmann, R.K. Szilagyi, K. Meyer, D.J. Mindiola, J. Am. Chem. Soc. 130 (2008) 3676.
[6] (a) C. Tejel, M.A. Ciriano, M. Pilar del Rio, D.G.H. Hetterscheid, N. Tsichlis i Spithas, J.M.N. Smits, B. de Bruin, Chem. Eur. J. 14 (2008) 10932;
(b) C. Tejel, M.P. del Rio, M.A. Ciriano, E.J. Reijerse, F. Hartl, S. Zalis, D.G.H. Hetterscheid, N. Tsichlis I Spithas, B. de Bruin, Chem. Eur. J. 15 (2009) 11878.
[7] (a) J.-P. Corbet, G. Mignani, Chem. Rev. 106 (2006) 2651;
(b) J.F. Hartwig, Acc. Chem. Res. 31 (1998) 852;
(c) J.F. Hartwig, Synlett (2006) 1283;
(d) J.F. Hartwig, Nature 455 (2008) 314.
[8] (a) R. Noyori, T. Ohkuma, Angew. Chem. Int. Ed. 40 (2001) 40;
(b) S.E. Clapham, A. Hadzovic, R.H. Morris, Coord. Chem. Rev. 248 (2004) 2201;
(c) K. Muñiz, Angew. Chem. Int. Ed. 44 (2005) 6622;
(d) J.S.M. Samec, J.-E. Bäckvall, P.G. Andersson, P. Brandt, Chem. Soc. Rev. 35 (2006) 237;
(e) B. Askevold, H.W. Roesky, S. Schneider, ChemCatChem 4 (2012) 307.
[9] F.R. Keele, Coord. Chem. Rev. 187 (1999) 121.
[10] (a) M.E. van der Boom, D. Milstein, Chem. Rev. 103 (2003) 1759;
(b) D. Morales-Morales, C. M.Jensen (Eds.), The Chemistry of Pincer Compounds, Elsevier, Amsterdam, 200; (c) J. Choi, A.H.R. McArthur, M. Brookhart, A.S. Goldman, Chem. Rev. 111 (2011) 1761.
[11] (a) L.-C. Liang, Coord. Chem. Rev. 250 (2006) 1152;
(b) J.I. van der Vlugt, J.N.H. Reek, Angew. Chem. Int. Ed. 48 (2009) 8832;
(c) C. Guananathan, D. Milstein, Acc. Chem. Res. 44 (2011) 588.
[12] Review articles: (a) D. Amoroso, T.W. Graham, R. Guo, C.W. Tsang, K. Abdur-Rashid, Aldrichimica Acta 41 (2008) 15;
(b) S. Schneider, J. Meiners, B. Askevold, Eur. J. Inorg. Chem. (2012) 412.
[13] (a) A. Friedrich, R. Ghosh, R. Kolb, E. Herdtweck, S. Schneider, Organometallics 28 (2009) 708;
(b) J. Meiners, A. Friedrich, E. Herdtweck, S. Schneider, Organometallics 28 (2009) 6331.
[14] A. Marziale, E. Herdtweck, J. Eppinger, S. Schneider, Inorg. Chem. 48 (2009) 3699.
[15] S. Park, A.L. Rheingold, D.M. Roundhill, Organometallics 10 (1991) 615.
[16] (a) F.G. Bordwell, Acc. Chem. Res. 21 (1988) 456;
(b) K. Abdur-Rashid, T.P. Fong, B. Greaves, D.G. Gusev, J.G. Hinman, S.E. Landau, A.J. Lough, R.H. Morris, J. Am. Chem. Soc. 122 (2000) 9155.
[17] (a) J.R. Fulton, M.W. Bouwkamp, R.G. Bergman, J. Am. Chem. Soc. 122 (2000) 8799;
(b) T. Büttner, F. Breher, H. Grützmacher, Chem. Commun. (2004) 2820;
(c) P. Maire, F. Breher, H. Schönberg, H. Grützmacher, Organometallics 24 (2005) 3207.
[18] J. Heinze, Angew. Chem. 96 (1984) 823.
[19] R. Dorta, H. Rozenberg, L.J.W. Shimon, D. Milstein, Chem. Eur. J. 9 (2003) 5237.
[20] (a) F.G. Bordwell, G.E. Drucker, H.E. Fried, J. Org. Chem. 46 (1981) 632;
(b) F.G. Bordwell, H.E. Fried, J. Org. Chem. 56 (1991) 4218.
[21] M.J. Frisch, G.W. Trucks, H.B. Schlegel, G.E. Scuseria, M.A. Robb, J.R. Cheeseman, J.A. Montgomery, T. Vreven, K.N. Kudin, J.C. Burant, J.M. Millam, S.S. Iyengar, J. Tomasi, V. Barone, B. Mennucci, M. Cossi, G. Scalmani, N. Rega, G.A. Petersson, H. Nakatsuji, M. Hada, M. Ehara, K. Toyota, R. Fukuda, J. Hasegawa, M. Ishida, T. Nakajima, Y. Honda, O. Kitao, H. Nakai, M. Klene, X. Li, J.E. Knox, H.P. Hratchian, J.B. Cross, V. Bakken, C. Adamo, J. Jaramillo, R. Gomperts, R.E. Stratmann, O. Yazyev, A.J. Austin, R. Cammi, C. Pomelli, J.W. Ochterski, P.Y. Ayala, K. Morokuma, G.A. Voth, P. Salvador, J.J. Dannenberg, V.G. Zakrzewski, S. Dapprich, A.D. Daniels, M.C. Strain, O. Farkas, D.K. Malick, A.D. Rabuck, K. Raghavachari, J.B. Foresman, J.V. Ortiz, Q. Cui, A.G. Baboul, S. Clifford, J. Cioslowski, B.B. Stefanov, G. Liu, A. Liashenko, P. Piskorz, I. Komaromi, R.L. Martin, D.J. Fox, T. Keith, M.A. Al-Laham, C.Y. Peng, A. Nanayakkara, M. Challacombe, P.M.W. Gill, B. Johnson, W. Chen, M.W. Wong, C. Gonzalez, J.A. Pople, Gaussian03 Rev. C.02, Gaussian Inc., Wallingford, CT, 2004.
[22] J.P. Perdew, K. Burke, M. Ernzerhof, Phys. Rev. Lett. 77 (1996) 3865.
[23] (a) D. Andrae, U. Häußermann, M. Dolg, H. Stoll, H. Preuß, Theor. Chim. Acta 77 (1990) 123;
(b) J.M.L. Martin, A. Sundermann, J. Chem. Phys. 114 (2001) 3408.
[24] (a) W.J. Hehre, R. Ditchfield, J.A. Pople, J. Chem. Phys. 56 (1972) 2257;
(b) M.M. Francl, W.J. Pietro, W.J. Hehre, J.S. Binkley, D.J. DeFrees, J.A. Pople, M.S. Gordon, J. Chem. Phys. 77 (1982) 3654;
(c) T. Clark, J. Chandrasekhar, G.W. Spitznagel, P. v. R. Schleyer, J. Comp. Chem. 4 (1983) 294.
[25] R. Dennington II, T. Keith, J. Millam, GaussView V4.1, Semichem Inc., Shawnee Mission, KS, 2007, p. 1.